Vol. 15(2), pp. 90-98, April-June, 2020
DOI: 10.5897/IJPS2020.4864
Article Number: B00067F63907
ISSN 1992-1950

http://www.academicjournals.org/IJPS

ACADEMIC JOURNALS

International Journal of Physical Sciences

Full Length Research Paper

Interpretation of aeromagnetic data over some parts of Sokoto Basin, Nigeria, using source parameter imaging and 3D Euler deconvolution methods

Suleiman Taufiq[1]*, Okeke, F. Nneka[2] and Obiora, N. Daniel[2]

[1]Department of Science, Waziri Umaru Federal Polytechnic, B/Kebbi, Kebbi State, Nigeria.
[2]Department of Physics and Astronomy, University of Nigeria, Nsukka, Nigeria.

Received 1 January, 2020; Accepted 9 March, 2020

This investigation is aimed at determining depth to the bottom of magnetic source and to reveal some certain geological features across Sokoto basin using source parameter imaging and 3D Euler deconvolution techniques. The investigation employed fifteen number aeromagnetic sheets covering longitude 4°30'E - 6°00E and latitude 11°00'N - 13°30'N. The total magnetic intensity of the area was subjected to reduction to magnetic equator using a geomagnetic inclination angle of 1.4°, declination of 1.7° and a standard deviation of 0.1. Similarly, the total magnetic intensity was also subjected to regional - residual separation using polynomial fitting of the second order, of the least square method. Consequently, the total magnetic intensity and the reduction to equator revealed intensities ranging from -67.16 to 118.27 nT and -58.33 to 119.21 nT/m, respectively. Similarly, the results from 3D Euler deconvolution revealed depths of 1.38, 2.14, 2.58 and 2.80 km for structural indexes of 0, 1, 2 and 3, respectively. Finally, the source parameter imaging result revealed a maximum depth of 1.65 km and a minimum of 0.1 km in the study area. The implication of these results is that, even if other conditions are met, the possibility of hydrocarbon exploration in the basin may be very marginal.

Key words: Aeromagnetic data, reduction to equation, Euler deconvolution, source parameter imaging, Sokoto basin.

INTRODUCTION

Sequel to the release of the of high resolution aeromagnetic data by the Nigerian Geological Survey Agency acquired between 2005 and 2010 with 500 m line spacing and 80 m terrain clearance for most parts of Nigeria, the need to re-subject the data across Sokoto basin to a more geophysical investigation becomes inevitable. Measurements involving the use of magnetic survey are used in estimating the geomagnetic field at any point on the earth's surface. The method is a non-destructive method and measures the susceptibility contrast of subsurface rocks. By delineating subsurface structures due to the difference in susceptibility, geological inferences/interpretations which include delineation of faults, fonds, lithology, and depth can be made. Determination of depth to causative magnetic sources or the sedimentary thickness is primarily a topic of research by geoscientists within the study area and environs.

*Corresponding author. E-mail: taufiq.suleiman.pg01826@unn.edu.ng, suleimantaufiq@gmail.com.

Spectral depth analysis has been quantitatively used by Umego (1990) to determine the depth of causative magnetic sources over Sokoto basin. An average sedimentary thickness of 1.67 km was observed by the authors. Shehu et al. (2004) and Adetona and Udensi (2007) also carried out spectral depth analysis of the Basin and revealed depths of ranges between 1.2 and 2.0 km. In the work of Bonde et al. (2014), the entire basin was subjected to basement depth estimation using spectral analysis. The authors revealed two prominent magnetization layers of depths varying from 0.04 to 0.95 km and 0.36 to 2.88 km for shallow and deeper sources, respectively. Others who have also used spectral analysis in estimating the sedimentary thickness of the basin are Kamba et al. (2017) with a shallow depth from 0.6 to 1.2 km and deeper depth from 2.5 to 3.2 km, Kamureyina (2019), revealed a shallow depth of 0.17 to 0.97 and a deeper source of 0.41 to 2.69 km.

In view of these several kinds of research made by different researchers/authors within the study area using spectral analysis technique, this study is therefore aimed at evaluating the sedimentary thickness of the Basin using a combined approach of Source parameter imaging and Euler deconvolution with a view to comparing the results with the previous works done in the Basin.

Geology and location of the study area

The Sokoto Basin is an embayment of the Iullemeden Basin and is located at the southeastern part of the Iullemeden Basin and northwest of Nigeria (Odebode, 2010). Found in the basin are sequences of sands, clay, some limestone and ironstone, and semi consolidated gravels. It consists of about 60% of the sedimentary and 40% of basement (Zboril, 1984). The sedimentary sequences are subdivided into late Jurassic to early Cretaxeous Illo and Gundumi Formation, the Maestrichtian Rima Group, the late Paleocene Sokoto Group and the Eocene-Miocene Gwandu Formation (Kogbe, 1989).

Kogbe (1989) described Sokoto basin as a series of crystalline massif rocks outcropping to the east and south of the basin consisting of granite gneisses, schist, phyllites, quartzites and some amphibolite, diorite, gabbro and marble of pre-Cambrian age. The lowlands and plains of the basement areas are sometimes covered on the surface by Quaternary sediments of Aeolian and fluvial origin especially along the flood plains of the major rivers and streams. The Basin lies between longitudes 3°E and 7°E and latitudes 10°N and 14°N. Figure 1 is the geologic map of the study area.

MATERIALS

Fifteen aeromagnetic maps with sheet number 9, 10, 11, 28, 29, 30, 50, 51, 52, 73, 74, 75, 96, 97 and 98, which are Dange, Sokoto, Rabah, Argungu, Dange, Gandi, Tambuwal, Gummi, Anka, Fokku, Danko, Gwanda, Shanga, Zuru, and Wasagu respectively were acquired from the Nigerian Geological Survey Agency (NGSA) Abuja. All the gridded data were saved and delivered in Oasis Montaj Geosoft raster file format. Each 1:100,000 topographical sheet covers an area of 3025 km^2 (55 x 55 km^2) totaling 45,375 km^2.

METHODS

Since total magnetic intensity normally displays gross interpretation limitation, enhancement is, therefore, necessary on it and was carried out. The enhancement was done in the spatial frequency domain by the introduction of Fast Fourier Transform. These include a reduction to the equator, regional and residual separation, and tilt derivatives. Subsequently, SPI and Euler deconvolution were carried out for depth estimation. A more elaborate description of the principle, theory, application, and formulation of these routines are described previously (Nabighian, 1972, 1984; Thompson, 1982; Thurston et al., 1999, 2002; Reeves, 2005; Nabighian et al., 2005; Whitehead and Musselman, 2008), but the present study only explained in brief.

Reduction to magnetic equator (RTE)

Reduction to the equator is used in low magnetic latitudes to centre the peak of magnetic anomalies over their sources, enhancing basement architecture including structural lineaments with its orientations thereby making the data easier to interpret without losing any geophysical meaning (Gilbert and Geldano, 1985). The TMI was reduced-to-equator in agreement with the International Geomagnetic Reference Field (IGRF) reduction technique using a geomagnetic inclination angle -1.4°, geomagnetic declination angle -1.7° and a standard deviation of 0.1. Equation 1 is the expression for RTE.

$$L(\theta) = \frac{\left[\sin(I) - i.\cos(I).\cos(D-\theta)\right]^2 \times (-\cos^2(D-\theta))}{\left[\sin^2(Ia) + \cos^2(Ia).\cos^2(D-\theta)\right] \times \left[\sin^2(I) + \cos^2(I).\cos^2(D-\theta)\right]} \quad (1)$$

If (/Ia/</I/), Ia = I.
Where, I = geomagnetic inclination Ia = Inclination for amplitude correction (never less than I), D = geomagnetic declination.

Regional/residual separation

The residual magnetic field of the study area was produced by subtracting the regional field from the total magnetic field using the polynomial fitting of second-order of least square method. Equation (2) was used in generating the algorithm for removal of regional data (Ugwu et al., 2013):

$$r = a_0 + a_1\left(x - x_{ref}\right) + a_2\left(y - y_{ref}\right) \quad (2)$$

where r is the regional field, x_{ref} and y_{ref} are the x and y coordinates of the geographic centre of the data set respectively; a_0, a_1 and a_2 are the regional polynomial coefficients.

Tilt derivative

This utilizes the ratio of the vertical derivative to the absolute value

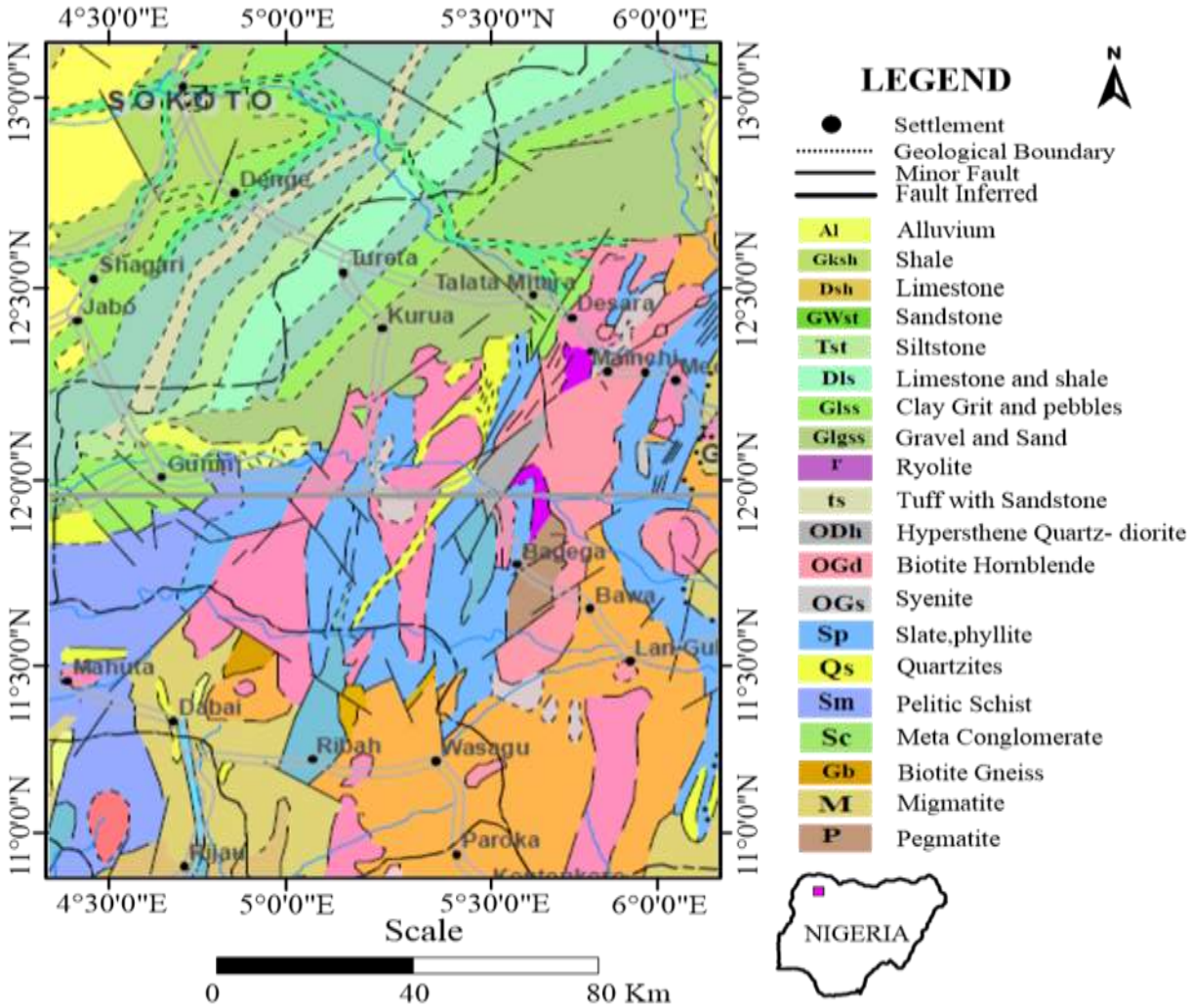

Figure 1. Geological map of the study area (After NGSA, 2009).

of the horizontal derivative; hence, it overcomes the problem of the shallow and deep sources (Eze et al., 2017). This is useful in mapping shallow basement structures and mineral exploration targets. Tilt derivative is defined as:

$$THDR = \sqrt{\left(\frac{\partial T}{\partial x}\right) + \left(\frac{\partial T}{\partial y}\right)} \quad (3a)$$

$$TDR = \tan^{-1}\left(\frac{1VDR}{THDR}\right) \quad (3b)$$

Where 1VDR and THDR are first vertical and total horizontal derivatives, respectively, of the total magnetic intensity T.

Source parameter imaging

This utilizes the relationship between source depth and the local wavenumber (K) of the observed field, which is calculated for any point within a grid of data via horizontal and vertical gradients (Thurston and Smith, 1997). The source parameter imaging (SPI) technique is represented mathematically (Thurston and Smith, 1997) as:

$$Depth = \frac{1}{K_{\max}} \quad (4a)$$

Where K_{max} is the peak value of the local wave number K over the step source. It can be shown
that:

$$K_{\max} = \sqrt{\left(\frac{\partial Tilt}{\partial x}\right)^2 + \left(\frac{\partial Tilt}{\partial y}\right)^2} \quad (4b)$$

where the tilt is given as:

$$Tilt = \arctan = \frac{\partial T / \delta z}{\left(\sqrt{\left(\frac{\partial T}{\partial x}\right)^2 + \left(\frac{\partial T}{\partial y}\right)^2}\right)} \quad (4c)$$

$$Tilt = \frac{\partial T / \partial z}{HGRAD} \quad (4d)$$

Where *HGRAD* is a horizontal gradient, *T* is total magnetic intensity, $\partial T/\partial x$, $\partial T/\partial y$, $\partial T/\partial z$ are the first order partial derivates of the total magnetic intensity (*T*) in x, y and z coordinates.

The ratio of the vertical gradient to the horizontal derivative shown in Equation (4) has been define as the tilt angle (Miller and Singh, 1994). The tilt angle acts as an automatic gain filter and is seen here as an excellent edge detector.

Euler deconvolution

The Euler deconvolution depth technique is basically based on the Euler's homogeneity equation. The magnetic field and its gradient are related to the location of the source of an anomaly, with the degree of homogeneity expressed as a "structural index". The structural index (SI) entails the degree of fall off of the field with distance from the causative source. The Standard 3D form of Euler's equation (Reid et al. 1990) can be defined as:

$$x\frac{\partial T}{dx} + y\frac{\partial T}{dy} + z\frac{\partial T}{dz} + \eta T = x_o\frac{\partial T}{dx} + y_o\frac{\partial T}{dy} + z_o\frac{\partial T}{dz} + \eta b \quad (5)$$

where x, y and z are the coordinates of a measuring point; x_o, y_o and z_o are the coordinates of the source location whose total field is detected at x, y and z. *b* is a base level, η is structural index and T is a potential field.

The method involves setting an appropriate SI value and using least-squares inversion to solve the equation for an optimum x_o, y_o, z_o and b. Also, an appropriate window size must be specified which consists of the number of cells in the gridded dataset to use in the inversion at each selected solution location.

RESULTS AND DISCUSSION

The enhancements/derivatives were generated in Oasis Montaj using the MAGMAP GX, while SPI and Euler deconvolution are essentially depth-estimation and were estimated using SPI GX and Euler GX respectively.

The Total Magnetic Intensity (TMI)

The TMI of the area shown in Figure 2 indicated magnetic intensities range between -67.16 nT to 118.27 nT. It revealed variations of highs and lows magnetic signature. The high magnetic anomalies which are probably attributes of igneous intrusion and shallower sediment (denoted with High) are found majorly around the Northwestern part of the study area, around Binji, Sokoto, and Argungu. The low magnetic anomalies which are associated with the sedimentary region are found within the Southeastern (Gwashi, Wasagu and Zuru areas), Northcentral (Dange and Gummi) and in the northwestern (part of Binji) of the study area. Another feature (yellow) which dominates the study area is the intermediary, it corresponds to granitic rocks.

Reduction to magnetic equator map and residual map

The RTE (Figure 3a) map exposes magnetic anomalies, discontinuities and minor fault lines. The fault lines are observed in NW, SE and SW of the study area. The discontinuities observed can be interpreted as contact between lithological units or fractures. The residual map (Figure 3b) indicated magnetic intensities range between -81.82 and 67.20 nT.

Tilt derivative

The RTE grid was subjected to Tilt Derivative (TDR) filter in order to determine the lineament, faults/joints, the boundaries of magnetic sources, the contacts and also to enhance strong and weak magnetic anomalies in the area. From Figure 4, few major fault systems were noticed on the image which is identified as F and trend NE-SW, NE-SE observed. The TDR map also showed a clear demarcation between low and high amplitude as indicated with letter D. The lower amplitude are areas characterized by Shale Awgu Group and granite, with amplitude range of 0.0004 to 0.0011 Rad while the high amplitude are areas characterized by migmatite, medium grain older granite and granite gneiss with amplitude range of 0.0049 to 0.0060 Rad.

Source parameter imaging (SPI)

The SPI map in Figure 5 reveals a maximum depth of 1.7 km occurring in the northern part of the study area and the least depth of 0.9 km. The SPI result obtained in the present investigation is in agreement with the work of Umego (1990) who obtained a maximum depth of 1.6 km using spectral analysis technique. The result is also in close agreement with the work of Shehu et al. (2004) and Ofor and Udensi (2014) who got maximum depths of 1.4 and 1.54 km respectively using spectral analysis. However, the present investigation is not in agreement with the work of Ofoha et al. (2016) who obtained a maximum depth of 3.4 km using the same SPI technique. Even though the average thickness obtained from the investigation of Ofoha et al. (2016) and the present study are in close agreement.

Euler deconvolution

Euler solutions were calculated according to the following parameters: Structural indexes of 0, 1, 2, and 3,

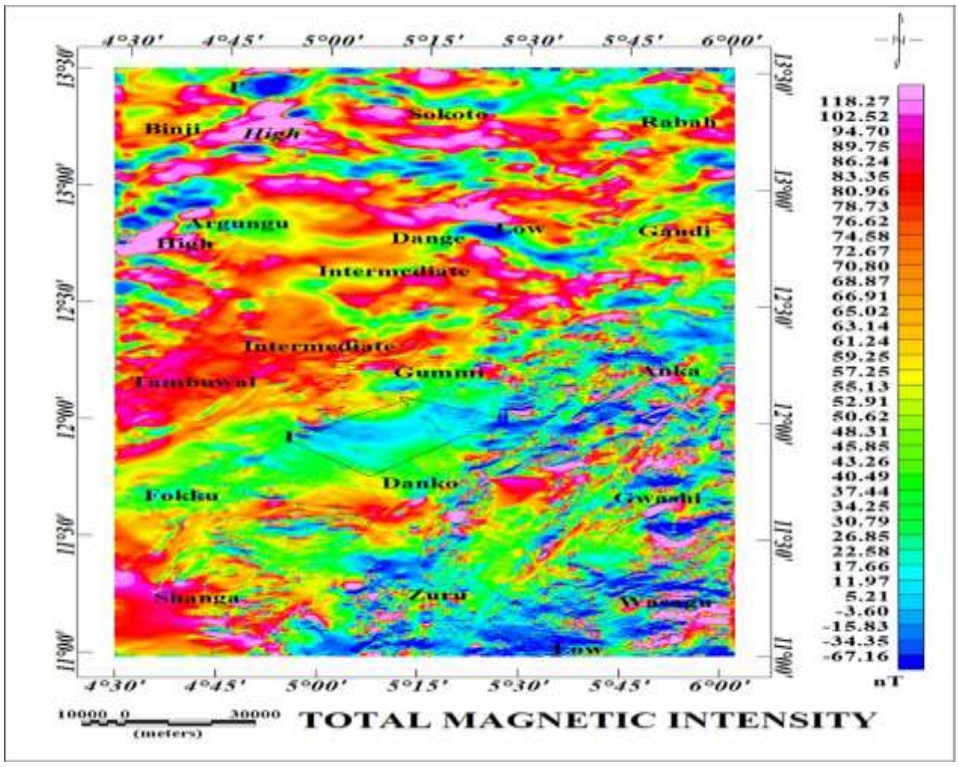

Figure 2. Total magnetic intensity indicating high, intermediate and low intensity with areas.

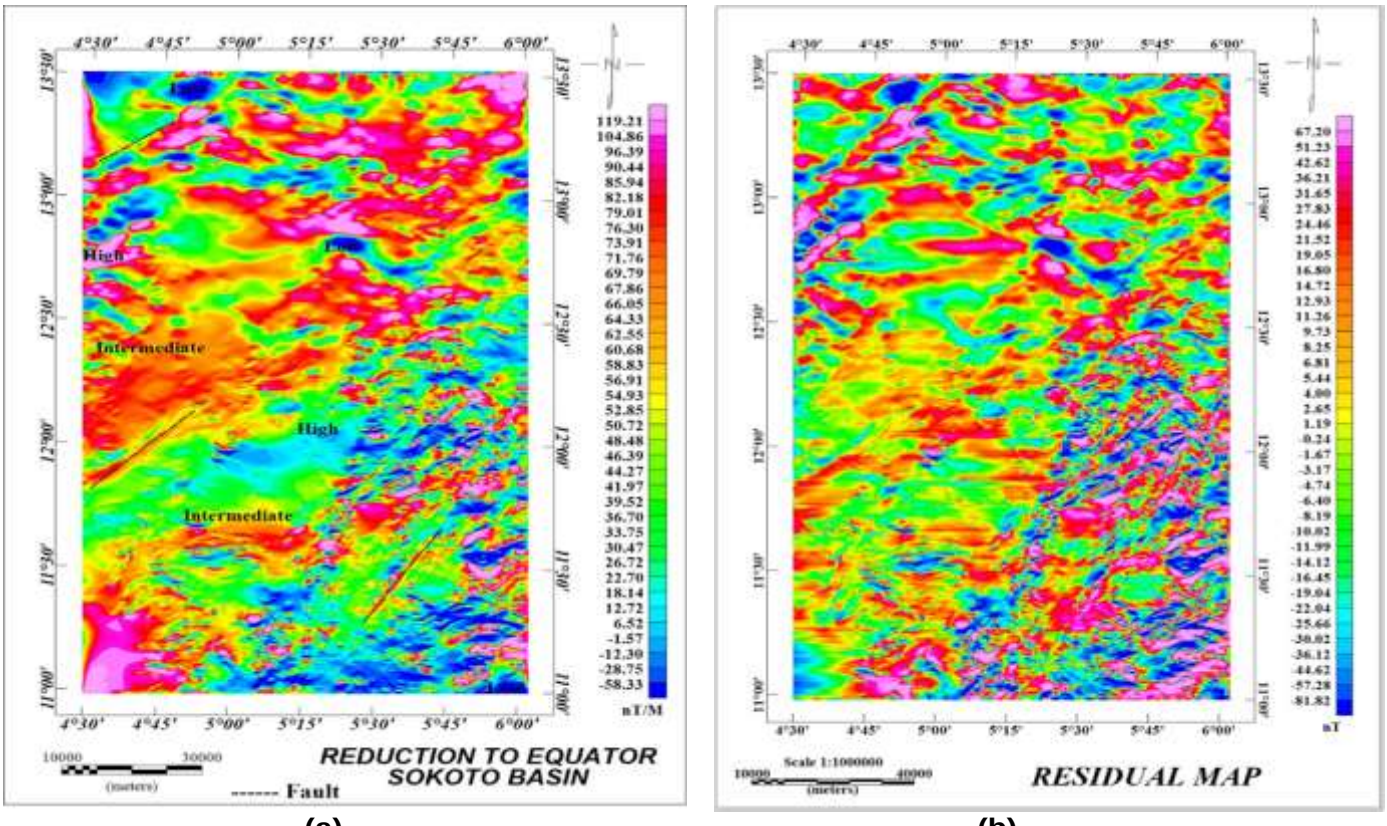

Figure 3. RTE map and residual map.

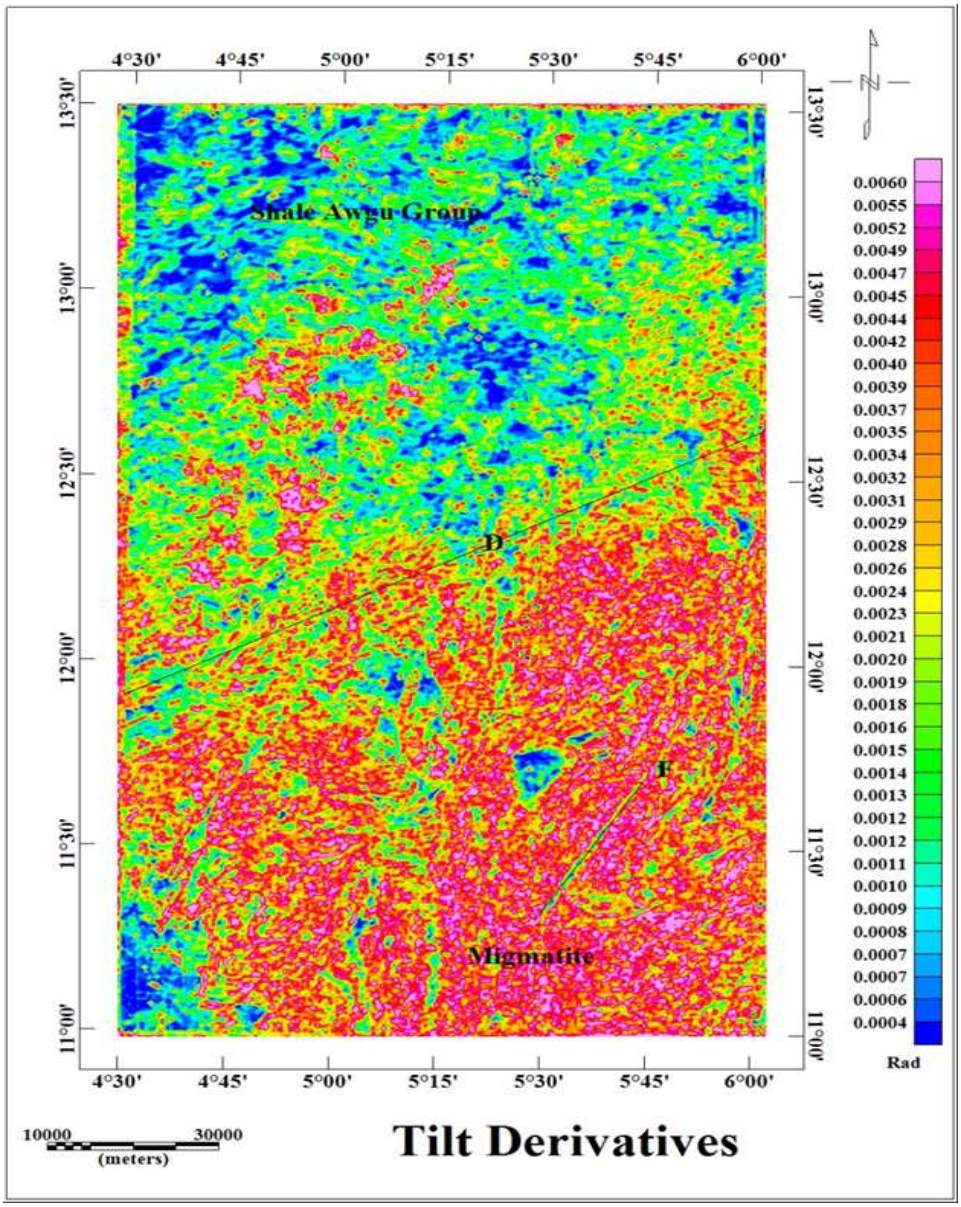

Figure 4. Tilt derivatives map.

maximum percentage depth are 15, while the window size is 10 (Figure 6). The structural indexes equals 0, 1, 2 and 3 allow highlighting the observed magnetic contacts, dykes, cylindrical pipe and sphere respectively over the study area. The Euler maps seem to be similar to that of the SPI maps (Figure 5) except that in some locations, the Euler maps lack solutions. The Euler deconvolution for a structural index of 0 (Figure 6a) revealed depths which ranges from 0.23 to 1.38 km while for the structural index of 1 and 2 (Figures 6b and c), the depths range from 0.20 to 2.14 km and 0.35 to 2.58 km respectively. Lastly, for the structural index of 3 (Figure 6d), depths of 0.50 to 2.80 km were observed as the least and maximum depth respectively.

Conclusion

Fifteen high resolution aeromagnetic data across Sokoto Basin has been subjected to depth estimation using source parameter imaging and 3D Euler deconvolution techniques.

The results obtained in the present investigation conforms favourably with the results of other researchers that used spectral analysis and old data acquired between 1974 and 1980. Consequently, the area can be generally characterized as a shallow area and therefore concealment of hydrocarbon may not be viable, hence, the area should be explored for mineral and geothermal potential.

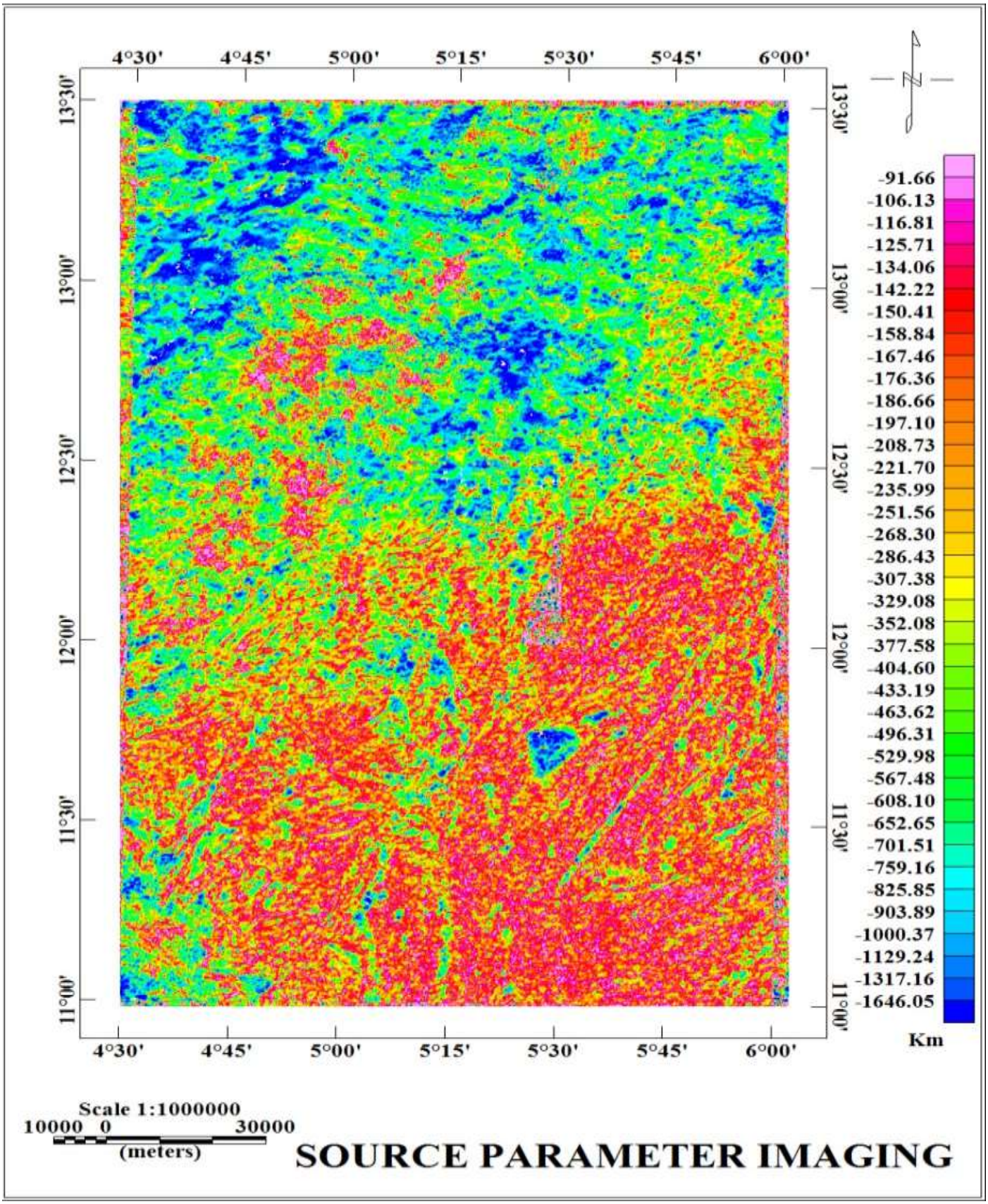

Figure 5. Source parameter imaging map.

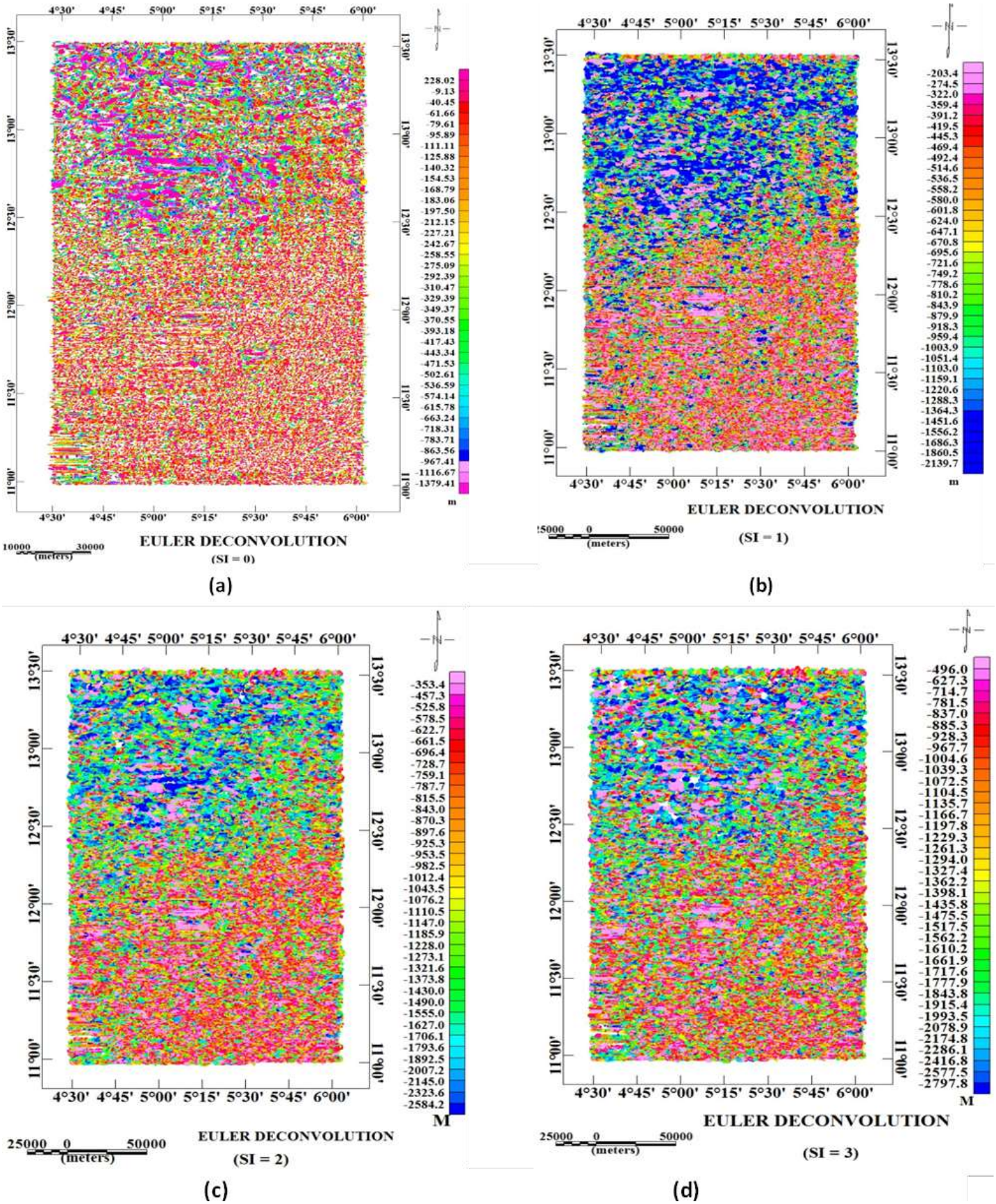

Figure 6. Maps of Euler deconvolution.

REFERENCES

Adetona AA, Udensi EE (2007). Spectral Depth Determination to Buried Magnetic Rocks under the Lower Sokoto basing using aeromagnetic Data. Nigeria Journal of Physics 19(2):275-283

Bonde DS, Rai JK, Joshua BW, Abbas M (2014). Basement depth estimates of Sokoto sedimentary basin, Northwestern Nigeria, using spectral depth analysis. Direct Research Journal of Chemistry and Material Science 2(2):21-26.

Eze MO, Mamah LI, Madu AJC, Leonard O (2017). Geological and structural interpretation of possible mineralization zones of part of Anambra basin and Southern Benue Trough using airborne geophysical data. International Journal of Research in Engineering and Applied Sciences 7(5):70-80.

Gilbert D, Geldano A (1985) A computer programme to perform transformations of gravimetric and aeromagnetic surveys. Computers and Geosciences 11:553-588.

Kamba AH, Muhammad S, Illo AG (2017). Basement Depth Estimates of some part of Lower Sokoto Sedimentary Basin, North-western Nigeria, Using Spectral Depth Analysis. International Journal of Marine, Atmospheric and Earth Sciences 6(1):1-9.

Kamureyina E (2019). Geothermal Study Over Sokoto Basin Northwestern, Nigeria. International Journal of Engineering Science Invention 8(05):34-48.

Kogbe CA (1989). Cretaceous and Tertiary of the Iullemmeden Basin in Nigeria in: C.A. Kogbe (eds.), Geology of Nigeria, pp. 377-421. Jos, Rock View Publ. Co.

Miller HG, Singh V (1994). Potential field tilt – a new concept for location of potential field sources. International Journal of Geophysics 32:213-217.

Nabighian MN (1972). The analytic signal of two-dimensional magnetic bodies with polygonal cross-section: Its properties and use for automated anomaly interpretation. Geophysics 37:507-517.

Nabighian MN (1984). Toward a three-dimensional automatic interpretation of potential field data via generalized Hilbert transforms: Fundamental relations. Geophysics 49:780-786.

Nabighian MN, Grauch VJS, Hansen RO, LaFehr TR, Li Y, Peirce JW, Phillips JD, Ruder ME (2005). The Historical Development of the Magnetic Method in Exploration. Geophysics 70(6):33-71.

Nigerian Geological Survey Agency (NGSA) (2009). Geological map of Nigeria. Map prepared by Nigerian Geological Survey Agency. 31 Shetima Mangono Crescent Utako District, Garki, Abuja.

Odebode MO (2010). Sokoto Basin, Northwest Nigeria. A Hand Book on Geology.

Ofoha CC, Emujakporue NG, Kiani MII (2016). Determination of Magnetic Basement Depth over Parts of Sokoto Basin, within Northern Nigeria, Using Improved Source Parameter Imaging (ISPI) Technique. World Scientific News 50:266-277.

Ofor NP and Udensi EE (2014). Determination of the Heat Flow in the Sokoto Basin, Nigeria using Spectral Analysis of Aeromagnetic Data. Journal of Natural Sciences Research 4(6):83-93.

Reeves CV (2005). Aeromagnetic Surveys, Principles, Practice and Interpretation; Geosoft 155 p.

Reid AB, Allsop JM, Granser H, Millet AJ, Somerton IW (1990). Magnetic interpretations in three dimensions using Euler deconvolution. Geophysics 55:80-91.

Shehu AT, Udensi EE, Adaniyi JO, Jonah SA (2004). Spectral Analysis of the Magnetic Residual Anomalies over the Upper Sokoto Basin, Nigeria. Zuma Journal of Pure and Applied Sciences l6(2):37- 49.

Thompson DT (1982). EULDPH – A new technique for making computer-assisted depth estimates from magnetic data. Geophysics 47:31-37.

Thurston JB, Smith RS (1997). Automatic conversion of magnetic data to depth, dip, and susceptibility contrast using the SPITM method. Geophysics 62(3):807-813.

Thurston J, Guillion JC, Smith RS (1999). Model independent depth estimation with the SPI method; 69th Annual International Meeting, SEG, Expanded Abstracts pp. 403-406.

Thurston J, Smith RS, Guillion JC (2002) A multi-model method for depth estimation from magnetic data. Geophysics 67:555–561.

Ugwu GZ, Ezema PO, Ezeh CC (2013). Interpretation of Aeromagnetic data over Okigwe and Afikpo Areas of the Lower Benue Trough, Nigeria. International Research Journal of Geology and Mining 3(1):1-8.

Umego MN (1990). Structural Interpretation of Gravity and Aeromagnetic Anomalies Over Sokoto Basin Northern-eastern Nigeria. Unpublished Ph.D Thesis, Ahmadu Bello University, Zaria, Nigeria.

Whitehead N, Musselman C (2008) Montaj Grav/Mag Interpretation: Processing, Analysis and Visualization System for 3D Inversion of Potential Field Data for Oasis montaj v6.3, Geosoft Incorporated, 85 Richmond St. W., Toronto, Ontario, M5H 2C9, Canada.

Zboril L (1984). Sketch map of oil-bearing structures. Geofyzika, Brno, Czechoslovakia P 94.